Brief Article

Isatin derived spirocyclic analogs with #-methylene-#-butyrolactone as anticancer agents: A structure activity rela-tionship study

Sandeep Rana, Elizabeth C. Blowers, Calvin Tebbe, Jacob I. Contreras, Prakash Radhakrishnan, Smitha Kizhake, Tian Zhou, Rajkumar N. Rajule, Jamie Arnst, Adnan R Munkarah, Ramandeep Rattan, and Amarnath Natarajan

J. Med. Chem., **Just Accepted Manuscript** • DOI: 10.1021/acs.jmedchem.6b00400 • Publication Date (Web): 14 Apr 2016

Isatin derived spirocyclic analogs with α-methylene-γ-butyrolactone as anticancer agents: A structure activity relationship study

Sandeep Rana[‡,Δ], Elizabeth C. Blowers[‡,Δ], Calvin Tebbe[§], Jacob I. Contreras[Δ], Prakash Radhakrishnan[Δ], Smitha Kizhake[Δ], Tian Zhou[¶], Rajkumar N. Rajule[†,Δ], Jamie L. Arnst [Δ], Adnan R. Munkarah[§], Ramandeep Rattan[§] and Amarnath Natarajan*[,Δ,¶,□,∞]

[Δ]Eppley Institute for Research in Cancer and Allied Diseases, Departments of [¶]Pharmaceutical Sciences and [□]Genetics Cell Biology and Anatomy, [∞]Fred and Pamela Buffett Cancer Center, University of Nebraska Medical Center, Omaha, Nebraska 68022, United States

[§]Division of Gynecology Oncology, Department of Women's Health and Josephine Ford Cancer Center, Henry Ford Hospital, Detroit, Michigan 48202, United States

ABSTRACT: Design, synthesis and evaluation of α-methylene-γ-butyrolactone analogs and their evaluation as anticancer agents is described. SAR identified a spirocyclic analog **19** that inhibited, TNFα-induced NF-κB activity, cancer cell growth and tumor growth in an ovarian cancer model. A second iteration of synthesis and screening identified **29** that inhibited cancer cell growth with low-μM potency. Our data suggests that an isatin-derived spirocyclic α-methylene-γ-butyrolactone is a suitable core for optimization to identify novel anticancer agents.

INTRODUCTION

Twenty one percent of currently marketed covalent drugs are used to treat cancer and several new covalent inhibitors are in clinical trials, suggesting the development of irreversible inhibitors as cancer therapeutics is making a strong comeback.[1-3] Covalent inhibitors were not fully explored as their perceived risk-reward ratio was heavily biased by concerns regarding their potential idiosyncratic effects. The resurgence of covalent inhibitors as cancer therapeutics can be attributed to the successful development of currently marketed irreversible inhibitors of enzyme active sites.[1] The current strategy for the development of covalent drugs for targeting oncogenic kinases is to append an electrophilic group to a reversible inhibitor. This electrophilic group on the reversible inhibitor then forms of a covalent bond with the sulfhydryl group of a non-catalytic cysteine residue peripheral to the kinase active site.[4] Here we report a biased approach for the identification of covalent inhibitors and their evaluation as anticancer agents.

Nuclear factor kappa B (NF-κB) is a transcription factor that plays a key role in innate and adaptive immune responses, inflammation, cell growth, and apoptosis.[5] In unstimulated cells, NF-κB is sequestered in the cytoplasm by its inhibitor, inhibitor of nuclear factor κB (IκBα). Upon stimulation with pro-inflammatory cytokines such as tumor necrosis factor alpha (TNFα), IκBα is phosphorylated by the IκB kinase β (IKKβ), ubiquitinated and rapidly degraded, allowing NF-κB dimers to translocate to the nucleus and activate transcription.[6] Immunohistochemistry (IHC) studies conducted with surgically resected tumor samples show that TNFα was found in ~50% of tumors suggesting that the NF-κB pathway is constitutively activated in a variety of cancers including pancreatic, breast and ovarian cancers and has been shown to contribute to anti-apoptosis, proliferation, tumor progression and chemoresistance.[7]

The key proteins in this pathway i.e., kinase IKKβ and the transcription factor NF-κB, have surface exposed cysteine residues. Cys[179] found in the activation loop of IKKβ is primed for targeting as it is between the serine residues 177 and 181. Phosphorylation of Ser[177] and Ser[181] results in the activation of IKKβ.[8] Cys38 in NF-κB (p65 subunit) plays an important role in its translocation to the nucleus to activate gene expression.[9] The sulfhydryl groups on Cys[179] of IKKβ and Cys[38] of NF-κB have been previously targeted using parthenolide, a sesquiterpene lactone natural product.[10,11] In a cell-based assay, we recently showed that parthenolide inhibits TNFα-induced-IKKβ-mediated NF-κB activity with low-μM potency.[12]

Natural products with the α-methylene-γ-butyrolactone functionality exhibit a wide-range of biological activities including anticancer and anti-inflammatory effects.[13-17] The available SAR with parthenolide analogs showed that the Michael acceptor in the α-methylene-γ-butyrolactone is critical for activity against the NF-κB pathway.[11] The Colby lab synthesized fluorinated amino derivatives of parthenolide and screened them for antiproliferative activities.[18,19] More recently, the Crooks lab generated a series of parthenolide and melampomagnolide-B analogs and screened them against a panel of 60 human cancer cell lines.[20-22] The α-methylene-γ-butyrolactone functionality was appended to small molecules to covalently link them to their biological target.[23,24] Compounds with α-methylene-γ-butyrolactone also show anticancer activities.[25-27] In the

studies presented here we have expanded on this general theme *via* synthesis of α-methylene-γ-butyrolactone containing analogs and screened them to identify pathway specific inhibitor. Multiple proteins in the NF-κB pathway have surface exposed cysteine residues; therefore, we screened our analogs in a TNFα-induced-IKKβ-mediated NF-κB reporter assay to identify covalent pathway specific inhibitors.

This exercise led to the identification of an isatin derived spirocyclic core with an α-methylene-γ-butyrolactone moiety (**19**) that inhibits the NF-κB pathway by covalently binding to IKKβ and NF-κB. This is the first report that identified a compound with spirocyclic α-methylene-γ-butyrolactone moiety as a NF-κB inhibitor. Analog **19** inhibits cancer cell growth *in vitro* and tumor growth in an orthotopic ovarian cancer model. Analog 19 is ~4-fold more stable in serum albumin when compared to parthenolide.

To explore this core structure we generated seven analogs with substitutions at different positions on the isatin-derived spirocyclic core and evaluated their ability to inhibit cancer cell growth. This led to identification of analog **29** with low-μM potency and ~2-20 fold more potency than parthenolide in a panel of cancer cell lines.

RESULTS AND DISCUSSION

We generated a biased library that features the α-methylene-γ-butyrolactone core using a reported two-step synthesis (Scheme 1)[28] and screened analogs at 10 μM (Figure 1B) in a cell-based luciferase assay (A549) that specifically reports on the ability of the compound to inhibit TNFα-induced IKKβ-mediated NF-κB activity.[12] ML-120B, a well-characterized IKKβ inhibitor, was used as a positive control.[29]

SCHEME 1. Synthesis of α-methylene-γ-butyrolactone containing spiroisatin analog **20**

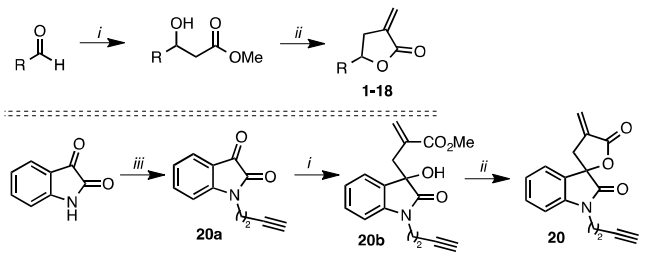

(i) Methyl- 2-(bromomethyl)acrylate, In powder, NH_4Cl, MeOH, 50 °C, 1h (ii) PTSA, CH_2Cl_2, 12h. (iii) 4-bromo-1-butyne, Cs_2CO_3, CH_3CN, 70 °C, 12h

The unsubstituted, mono- and di-substituted phenyl compounds (**2-10**) had modest activity (25-50% inhibition) with no clear SAR. Pyridine substitution (**11**) resulted in decreased activity (< 25% inhibition) while a bulky bromo group *ortho* to the nitrogen in **12** resulted in the recovery of activity (~50% inhibition). Interestingly introducing a second α-methylene-γ-butyrolactone in **13** did not increase the activity. In the bicyclic fused aryl ring systems unsubstituted 1- and 2-napthyl substituted analogs (**14** and **18**) had modest activity (~50% inhibition) while the 4-quinolinyl substitution resulted in an inactive compound (**15**). The methoxy substitution at the 2-position of 1-napthyl analog (**16**) was tolerated however a bigger benzyloxy substitution at the same position (**17**) resulted in reduced activity (< 25% inhibition). The spirocyclic analogs (**19** and **20**) in which the α-methylene-γ-butyrolactone is rigid had activities (~75% inhibition) comparable to the ML-120B indicating that rigidification of the Michael acceptor is a favorable feature.

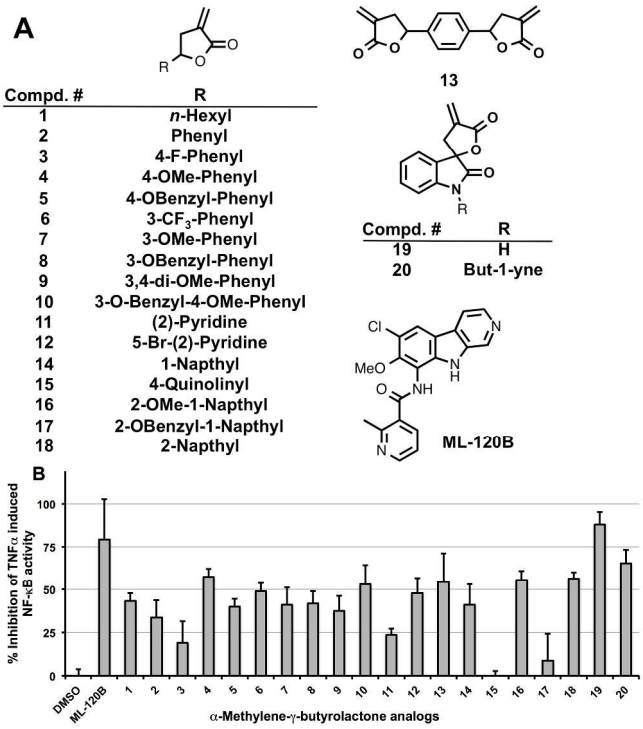

FIGURE 1. (A) Focused library of α-methylene-γ-butyrolactone analogs and the IKKβ inhibitor ML-120B (B) A cell-based screen (A549) that reports on the ability of the inhibitors to specifically block TNFα-induced IKKβ-mediated NF-κB activity.

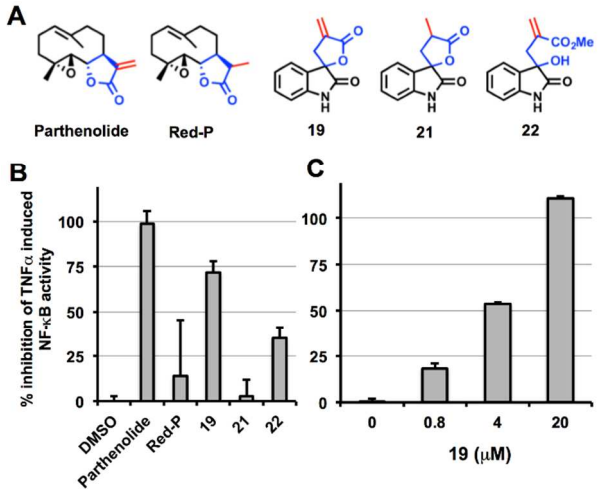

FIGURE 2. (A) Structure of Parthenolide, reduced Parthenolide and isatin analogs (B) Evaluation of inhibitors

in TNFα-induced NF-κB activity assay (C) Dose-response study with analog **19.**

To determine if the Michael acceptor is critical for activity, we tested the reduced spirocyclic compound that lacks the Michael acceptor **(21)** and compared it with Parthenolide and reduced Parthenolide analog (Red-P) (Figure 2A). At 10 μM, analog **19** showed good activity (> 70% inhibition) while reduced analog **21** was inactive (~ 5% inhibition), demonstrating that the Michael acceptor in **19** is critical for NF-κB inhibitory activity. Parthenolide showed remarkable activity (> 95% inhibition) while Red-P was ~4 fold less active (~ 20% inhibition) (Figure 2B).[11] To confirm whether rigidification indeed resulted in increased NF-κB inhibition, the isatin derived acyclic analog **(22)** was screened under identical conditions. Acyclic analog **22** was ~2 fold less active than the cyclized version (**19**) suggesting that rigidification indeed increases activity against the NF-κB pathway proteins. In a dose-response study, analog **19** had low-μM (IC_{50} ~ 4μM) inhibitory activity in the TNFα-induced IKKβ-mediated NF-κB activity assay (Figure 2C), which is comparable to Parthenolide (IC_{50} = 4.7 ± 1.5 μM).[12] To summarize, our synthesis and screening effort identified an isatin derived spirocyclic compound with the α-methylene-γ-butyrolactone as a potent NF-κB inhibitor. The acyclic analog **22** adopts multiple conformations when compared to the rigidified analog **19** and therefore could bind to additional targets, which explains the increased the NF-κB inhibitory activity observed with **19**.

One of the limitations with the use of parthenolide is the short half-life in serum. A recent study characterized the covalent binding of parthenolide through the α-methylene-γ-butyrolactone to the free cysteine (34) residue of serum albumin by MS analyses. They also determined the half-life of parthenolide to be ~37 minutes.[30] To determine the stability of our analog 19 we conducted a head-to-head comparison of analog **19** and parthenolide for serum albumin binding using HPLC (Figure S1). Our results show that half-life of **19** is 290 min as compared to 66 min for parthenolide indicating the spirocyclic disposition in **19** as opposed to a fused disposition in parthenolide could contribute to the observed increased serum stability.

Next, we used click chemistry[31] to determine if compound **19** indeed irreversibly binds to IKKβ and NF-κB. Recombinant IKKβ and NF-κB (p65) were incubated with analog **20,** which is analog **19** with an alkyne linker, for 1h at room temperature. Rhodamine azide and click reagents were added to the reaction mixture and incubated for an additional hour. At the end of the second hour, the mixture was subjected to SDS PAGE and the gel was imaged using the Typhoon 9410 Variable Mode Imager, an imager that produces digital images of fluorescent samples. The data summarized in Figure 3A shows fluorescent bands at molecular weights that correspond to IKKβ and NF-κB (p65 protein truncated at C-terminus and has L159V, P180S, F309S, A439V and V462M mutations runs at ~50 kDa – accession no. AAA36408) demonstrating that analog **20** is a covalent inhibitor of IKKβ and NF-κB. To determine if this is a Cys adduct we conducted a HPLC study wherein Boc protected Cys or Lys amino acids incubated with analog **19 (data not shown).** Our results showed that analog 19 reacts with only Cys and not Lys suggesting a Cys adduct.

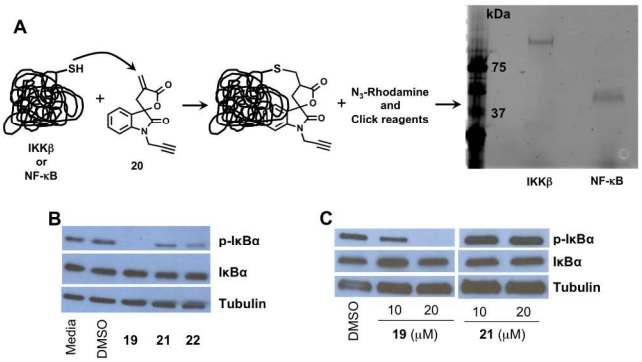

FIGURE 3. (A) Schematic of click chemistry used to demonstrate covalent binding (left) and covalent binding of **20** to IKKβ and p65 via click chemistry (right) (B) Inhibition of IKKβ kinase activity determined by Western blot analyses in MDA-MB-231 cells and (C) MiaPaCa2 cells.

To determine if covalent binding to IKKβ results in the inhibition of the kinase activity of IKKβ, cancer cells were incubated with analogs **19**, **21** and **22** for 2h. The cells were lysed and the proteins were separated on SDS PAGE, transferred to a membrane and probed with total and phosphospecific IκBα antibodies. Since IκBα is a substrate of IKKβ, inhibition of the kinase activity of IKKβ should result in reduced IκBα phosphorylation. Indeed we observed a complete inhibition of IκBα phosphorylation in cells treated with **19** but no inhibition of IκBα phosphorylation in cells treated with the reduced compound **21** that lacks the Michael acceptor (Figure 3B and C). Interestingly the acyclic analog **22** showed partial inhibitory activity (Figure 3B), which indicates that rigidification of the Michael acceptor results in increased inhibition of IKKβ.

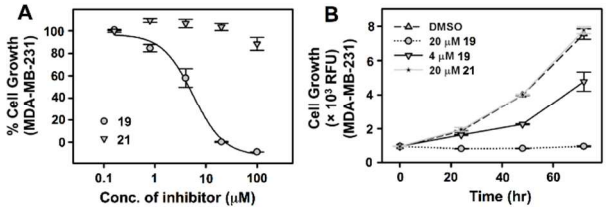

FIGURE 4. Dose-dependent (A) and time-dependent (B) effects on the growth of breast cancer cells by analogs **19** and **21.** Cell viability was assessed using PrestoBlue dye after 3 days treatment.

To determine if the IKKβ-NFκB inhibitory activity translates to anticancer activity, we subjected a panel of cancer cell lines to **19**, **21** and three previously reported IKKβ inhibitors 13-197,[32] Bayer VIII and TPCA1.[33-36] Analog **19** showed dose and time dependent inhibition of cancer cell growth while analog **21** did not (Figure 4A and 4B) further demonstrating that the Michael acceptor is critical for anticancer activity. Importantly, the growth inhibitory activity of **19** was comparable to known IKKβ inhibitors (Table S1).

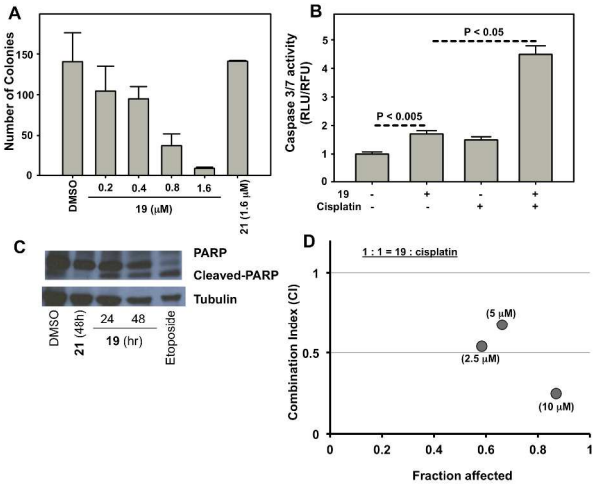

FIGURE 5. (A) Dose-dependent effects on colony formation of HeLa cells by analogs **19** and **21** (B) Caspase 3/7 activity induced by **19**, cisplatin and the combination in SKOV3 cells (C) The effects of **19**, **21** and Etoposide (positive control) on PARP cleavage in HeLa cells (D) A combination index (CI) versus fraction affected plot demonstrating synergistic growth inhibition with **19** and cisplatin $^{*}p < 0.05$ vs. control.

The ability of analog **19** and **21** to inhibit colony formation was accessed using a clonogenic assay. Cells were sparsely plated and allowed to grow in the presence or absence of **19** or **21** for 7 days. Colonies were then stained using crystal violet and quantified (Figure 5A). In the plates treated with **19,** we observed a dose-dependent decrease in the number of colonies while no such effect was observed with **21**. This demonstrates that the Michael acceptor functionality is critical for **19** to inhibit colony formation.

Inhibition of the NF-κB pathway has been explored as a therapeutic strategy to sensitize cancers to current chemotherapeutics.[37] The NF-κB inhibitor BAY 11-7085 that targets the NF-κB pathway proteins through covalent inhibition via its Michael acceptor sensitizes ovarian cancer cells to cisplatin-induced apoptosis.[38] Two key events during apoptosis are the activation of caspase 3/7 and poly (ADP-ribose) polymerase (PARP) cleavage. In cells treated with **19** we observed modest induction of caspase 3/7 by itself and synergistic induction in the presence of cisplatin (Figure 5B). This is consistent with reports that implicate activation of NF-κB in chemoresistance.[39] We also observed decreased/cleaved PARP in cells treated with **19**. Importantly no such effects with **21** treated cells (Figure 5C and Figure S2) were observed.

In order to determine if the observed synergistic induction of caspase 3/7 leads to growth inhibition, we subjected ovarian cancer cells to either **19** or cisplatin alone and their combination and monitored their effects on the cancer cell growth over a 3-day period (Figure 5D). The combination index (CI) values for the various combinations were derived from median effect plot and dose effect curves (Figure S3) using calcusyn (biosoft.com). CI < 1 indicates synergism, CI = 1 indicates additive effects and CI > 1 indicates antagonism.[40] Concentration combinations of **19** and cisplatin in the 1-10 μM range had CI < 1 indicating synergistic inhibition of ovarian cancer cell growth (Figure 5D). These studies demonstrate that **19** sensitizes cancer cells to cisplatin induced apoptosis and demonstrates synergism in the low-μM ranges with cisplatin toward the inhibition of ovarian cancer cell growth.

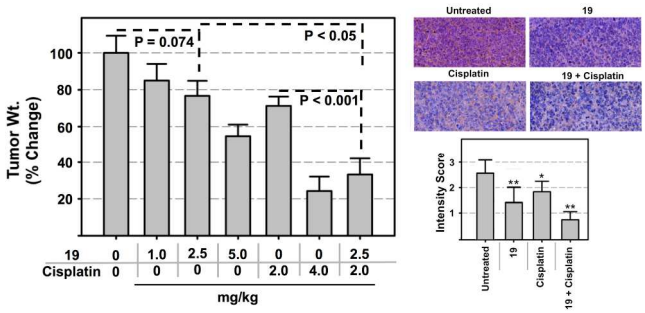

FIGURE 6. Dose-dependent effects on ovarian (A2780) tumor growth by analog **19**, cisplatin and the combination in an orthotopic model of ovarian cancer (left) and NF-κB(p65) staining of the excised tumors (right top) and quantification (right bottom) (n=10) $^{**}p < 0.01$, $^{*}p < 0.05$.

Our *in vitro* studies clearly demonstrate the anticancer effects induced by **19** are dependent on the presence of the Michael acceptor. We next investigated if these effects translate to an ovarian cancer mouse model.[41]

Our first goal was to determine if analog **19** has anticancer activity as a single agent and to define an optimal dose for both cisplatin and **19** in an orthotopic ovarian cancer model.[42,43] Ovarian cancer cells (A2780) were injected into the peritoneal cavity of nude mice and the tumors were allowed to establish. On day 3, mice were divided into four groups and the groups were treated with vehicle, 1, 2.5 or 5 mg/kg of **19,** the dose and route of administration were selected based on literature reports with parthenolide.[44-46] The mice were treated intraperitoneally 5 days a week for 4 weeks. At the end of the study the mice were sacrificed and the tumor weights determined. None of the mice treated with **19** showed any overt toxicity. A dose dependent effect on tumor growth (~ 10 – 40%) was observed in mice treated with **19**. A ~40% reduction in tumor weights in mice treated with **19** at the highest dose (5 mg/kg). The ~10% reduction in tumor growth at 1 mg/kg is consistent with the effects observed with parthenolide at an equivalent dose in the prophylactic metastasis study.[45] Consistent with our previous studies, we observed a ~25% reduction of tumor weights in mice treated with cisplatin (2 mg/kg) when compared to the controls (Figure 6A).[41]

To determine if **19** can chemosensitize ovarian tumors to cisplatin, we performed a follow up study in which mice were treated with 2.5 mg/kg of **19** (resulted in ~21% reduction in tumor growth bar #3 Figure 6A) and 2 mg/kg of cisplatin (resulted in ~30% reduction in tumor growth bar #5 Figure 6A). Therefore, a reduction of > 51% in tumor growth with the combination of 2.5 mg/kg of **19** and 2.0 mg/kg of cisplatin will indicate synergism. Indeed the combination was synergistic with ~65% (bar #7 Figure 6A) reduction in tumor weights compared to the controls. The reduction of tumor weights by treatment with 19 + cisplatin is significant compared to treatment with either drug alone (One-way ANOVA, P < 0.001). These studies clearly demonstrate that analog **19** has anticancer activity as a single agent and also demon-

strates the ability to chemosensitize ovarian tumors to cisplatin (Figure 6A).

To determine if **19** affects NF-κB (p65) levels and NF-κB regulated proteins (Mcl-1) in the tumors, we conducted IHC studies with p65 and Mcl-1 antibodies with the excised tumor tissue. IHC studies showed reduced p65 staining in tumors of animals treated with **19** and cisplatin individually and the combination (Figure 6B). Similar effects were observed in Mcl-1 levels (Figure S4). These studies suggest that the antitumor effects of **19** *in vivo* are mediated by the inhibition of the NF-κB pathway.

Since, *in vitro* and *in vivo* studies clearly demonstrate the anticancer effects of compound **19**, we functionalized the spirocyclic oxindole core with substitutions at various positions to generate seven additional analogs (Figure 7). We screened these for inhibition of cancer cell growth in A2780 cell lines (Table 1). In this cell line we observed a ~four-fold higher potency in cell growth inhibition with **19** compared to parthenolide which correlates with ~ 4-fold higher serum stability.

Alkylation (**20**, **23, 24**) of the nitrogen atom on the oxindole had modest effects on the growth inhibitory activity**.** Analog **25** with a phenyl substitution on the lactone ring did not have a significant effect on the activity. Likewise, substitutions at 4-7 positions (**26**-**29**) on the phenyl ring of the oxindole had modest effects when compared to **19** on the growth of A2780 cells. Only methyl substitutions at the both 4- and 7- positions of the oxindole (**29**) showed > 2-fold improvement in the growth inhibitory effects when compared to analog **19**. As expected, the corresponding reduced spirocyclic analog **30** was inactive (IC_{50} > 100 μM). Importantly, under our assay conditions, the growth inhibitory activity of **29** was ~13 fold better (IC_{50} values 1.0 μM vs. 12.9 μM) than parthenolide and ~ 20 fold better than ibrutinib. Surprisingly, reducing the Michael acceptor in ibrutinib (**Red-I**) did not alter the growth inhibitory effects. However, reduction of the Michael acceptor in parthenolide resulted in loss of activity (Table 1, Figure S5). Although limited in number, this preliminary study clearly demonstrates that the spirocyclic oxindole core with the α-methylene-γ-butyrolactone core can be functionalized to improve biological activity and possible drug like properties.

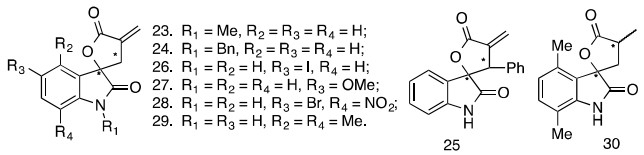

FIGURE 7. Focused library of substituted α-methylene-γ-butyrolactone – oxindole analogs.

TABLE 1. Inhibition of A2780 cancer cell growth by substituted α-methylene-γ-butyrolactone – oxindoles.

Analogs	EC_{50} values (μM)	Analogs	EC_{50} values (μM)
20	5.5 ± 0.58	19	2.3 ± 1.4
23	3.9 ± 0.45	29	1.0 ± 0.16
24	2.7 ± 0.23	30	>100
25	3.8 ± 0.21	ibrutinib	20.1 ± 1.26
26	2.2 ± 0.24	Red-I	15.2 ± 1.11
27	3.1 ± 0.32	parthenolide	12.9 ± 0.72
28	2.0 ± 0.12	Red-P	>100

We also compared the efficacy of analog **29**, its reduced analog **30**, parthenolide, reduced parthenolide (Red-P), ibrutinib and reduced ibrutinib (Red-I) in a panel of cancer cell lines (Table 2, Figure S6). Compound **29** was ~2-10 fold more potent than parthenolide and ~5-20 fold more potent than ibrutinib. Reduced compounds 30 and Red-P resulted in >10-fold loss of activity. However, reduced ibrutinib (Red-I) showed modest improvement in the growth inhibitory activity when compared to ibrutinib in all the lines. At the present time, we do not have an explanation for the results observed with ibrutinib and its reduced analog. On the other hand the cell-based activity of both parthenolide and **29** are largely dependent on the presence of the Michael acceptor.

TABLE 2. Inhibition of HeLaGFP, MiaPaCa-2 and SW480 cancer cell growth.

Inhibitors	IC_{50} ± SEM (μM)		
	HeLaGFP	MiaPaCa-2	SW480
Ibrutinib	16.8 ± 1.7	16.6 ± 2.4	25.6 ± 0.3
Red-I	15.1 ± 0.1	8.2 ± 1.4	13.4 ± 0.2
Parthenolide	5.7 ± 3.3	9.8 ± .05	15.3 ± 0.1
Red-P	66.1± 1.9	84.3 ± 11.1	>100
29	3.2 ± 0.03	0.9 ± 0.1	1.2 ± 0.2
30	>100	>100	>100

In conclusion, a cell-based based pathway screen with a focused library of α-methylene-γ-butyrolactone containing-analogs led to the identification of the isatin derived spirocyclic analog **19** as a potent inhibitor of TNFα-induced IKKβ-mediated NF-κB activation. SAR studies revealed that rigidification of the α-methylene-γ-butyrolactone and the Michael acceptor in the spirocyclic system are critical features required for activity. Changing the context of the α-methylene-γ-butyrolactone from a fused to a spirocyclic system could explain the increased stability of 19 in serum when compared to parthenolide. Using click chemistry we show that the inhibition of TNFα-induced IKKβ-mediated NF-κB activation is due to covalent binding of **19** to IKKβ and NF-κB. Analog **19** inhibited the phosphorylation of IκBα in cancer cells and exhibited anticancer activities that was comparable to known IKKβ inhibitors. On the other hand, analog **21,** a reduced form of **19,** was inactive in all the assays. Analog **19** inhibits ovarian tumor growth as a single agent and sensitizes ovarian tumors to cisplatin in an orthotopic model. Our studies clearly demonstrate that α-methylene-γ-butyrolactone containing spirocyclic oxindole analog **19** phenocopies the effects of natural product parthenolide. A second iteration of synthesis and screening led to the identification of a dimethyl analog **29,** which inhibited cancer cell growth with low-μM potency. Depending on cell lines, analog **29** was ~2-20 fold better than parthenolide. Studies to expand the SAR of α-methylene-γ-butyrolactone containing spirocyclic oxindole analogs for the identification of suitable pre-therapeutic lead compounds with anticancer effects are currently underway and the results from these studies will be reported in due course.

ASSOCIATED CONTENT

SUPPORTING INFORMATION

The supporting Information is available free of charge via the Internet at http://pubs.acs.org. Experimental for western blotting, cell viability assay, kB-luciferase assay, click chemistry, PARP cleavage, Caspase 3/7 assay, colony formation assay, mouse studies, Immunohistochemistry, synthetic procedures, NMR spectra.

AUTHOR INFORMATION

Corresponding Author

A.N.: phone, +402 559 3793; fax, +402 559 8270; E-mail, anatarajan@unmc.edu.

Present Addresses

†Ashland Inc., 601-608, Plot No. 17-18, Platinum Techno Park Sector 30-A, Vashi, Navi Mumbai, India

Author Contributions

‡ Equal contribution

ACKNOWLEDGMENT

This work was supported in part by CA182820, CA127297, Nebraska Research Initiative to A.N., LB506 to P.R. and DOD to R.R. We would like to thank Ed Ezell for NMR, Krishna Kattel for Mass spectrometry and the Natarajan lab members for helpful discussions. We would like to thank Fred & Pamela Buffett Cancer Center Support Grant (P30CA036727) for NMR core facility.

ABBREVIATIONS

SAR, Structure Activity Relationship; TNFα, tumor necrosis factor alpha; NF-κB, Nuclear factor kappa B; IκBα, inhibitor of nuclear factor κB; IKKβ, IκB kinase β; PARP, poly ADP ribose polymerase; IHC, immunohistochemistry.

REFERENCES

1. Singh, J.; Petter, R. C.; Baillie, T. A.; Whitty, A. The resurgence of covalent drugs. *Nat. Rev. Drug Discov.* **2011,** *10*, 307-317.
2. Liu, Q.; Sabnis, Y.; Zhao, Z.; Zhang, T.; Buhrlage, S. J.; Jones, L. H.; Gray, N. S. Developing irreversible inhibitors of the protein kinase cysteinome. *Chem. Biol.* **2013,** *20*, 146-159.
3. Kalgutkar, A. S.; Dalvie, D. K. Drug discovery for a new generation of covalent drugs. *Expert Opin. Drug Discov.* **2012,** *7*, 561-581.
4. Dou, D.; Park, J. G.; Rana, S.; Madden, B. J.; Jiang, H.; Pang, Y. P. Novel selective and irreversible mosquito acetylcholinesterase inhibitors for controlling malaria and other mosquito-borne diseases. *Sci. Rep.* **2013,** *3*, 1068.
5. Oeckinghaus, A.; Ghosh, S. The NF-kappaB family of transcription factors and its regulation. *Cold Spring Harb. Perspect. Biol.* **2009,** *1*, a000034.
6. Liu, F.; Xia, Y.; Parker, A. S.; Verma, I. M. IKK biology. *Immunol. Rev.* **2012,** *246*, 239-253.
7. Lee, D. F.; Kuo, H. P.; Chen, C. T.; Hsu, J. M.; Chou, C. K.; Wei, Y.; Sun, H. L.; Li, L. Y.; Ping, B.; Huang, W. C.; He, X.; Hung, J. Y.; Lai, C. C.; Ding, Q.; Su, J. L.; Yang, J. Y.; Sahin, A. A.; Hortobagyi, G. N.; Tsai, F. J.; Tsai, C. H.; Hung, M. C. IKK beta suppression of TSC1 links inflammation and tumor angiogenesis via the mTOR pathway. *Cell* **2007,** *130*, 440-455.
8. Byun, M. S.; Choi, J.; Jue, D. M. Cysteine-179 of IkappaB kinase beta plays a critical role in enzyme activation by promoting phosphorylation of activation loop serines. *Exp. Mol. Med.* **2006,** *38*, 546-552.
9. Garcia-Pineres, A. J.; Lindenmeyer, M. T.; Merfort, I. Role of cysteine residues of p65/NF-kappaB on the inhibition by the sesquiterpene lactone parthenolide and N-ethyl maleimide, and on its transactivating potential. *Life Sci.* **2004,** *75*, 841-856.
10. Govindachari, T. R. J., B. S.; Kamat, V. N. Structure of parthenolide. *Tetrahedron* **1965,** *21*, 1509-1519.
11. Kwok, B. H.; Koh, B.; Ndubuisi, M. I.; Elofsson, M.; Crews, C. M. The anti-inflammatory natural product parthenolide from the medicinal herb Feverfew directly binds to and inhibits IkappaB kinase. *Chem. Biol.* **2001,** *8*, 759-766.
12. Bryant, V. C.; Kishore Kumar, G. D.; Nyong, A. M.; Natarajan, A. Synthesis and evaluation of macrocyclic diarylether heptanoid natural products and their analogs. *Bioorg. Med. Chem. Lett.* **2012,** *22*, 245-248.
13. Ramachandran, P. V.; Yip-Schneider, M.; Schmidt, C. M. Natural and synthetic alpha,beta-unsaturated carbonyls for NF-kappaB inhibition. *Future Med. Chem.* **2009,** *1*, 179-200.
14. Kempema, A. M.; Widen, J. C.; Hexum, J. K.; Andrews, T. E.; Wang, D.; Rathe, S. K.; Meece, F. A.; Noble, K. E.; Sachs, Z.; Largaespada, D. A.; Harki, D. A. Synthesis and antileukemic activities of C1-C10-modified parthenolide analogues. *Bioorg. Med. Chem.* **2015,** *23*, 4737-4745.
15. Khazir, J.; Riley, D. L.; Chashoo, G.; Mir, B. A.; Liles, D.; Islam, M. A.; Singh, S. K.; Vishwakarma, R. A.; Pilcher, L. A. Design, synthesis and anticancer activity of Michael-type thiol adducts of alpha-santonin analogue with exocyclic methylene. *Eur. J. Med. Chem.* **2015,** *101*, 769-779.
16. Qin, X. Y.; Chen, B. Y.; Fu, J. J.; Shan, L.; Lei, X. G.; Zhang, W. D. Synthesis, cytotoxicity and inhibition of NO production of ivangustin enantiomer analogues. *Eur. J. Med. Chem.* **2015,** *102*, 256-265.
17. Xu, Y. Z.; Gu, X. Y.; Peng, S. J.; Fang, J. G.; Zhang, Y. M.; Huang, D. J.; Chen, J. J.; Gao, K. Design, synthesis and biological evaluation of novel sesquiterpene mustards as potential anticancer agents. *Eur. J. Med. Chem.* **2015,** *94*, 284-297.
18. Woods, J. R.; Mo, H.; Bieberich, A. A.; Alavanja, T.; Colby, D. A. Fluorinated amino-derivatives of the sesquiterpene lactone, parthenolide, as (19)f NMR probes in deuterium-free environments. *J. Med. Chem.* **2011,** *54*, 7934-7941.
19. James R. Woods; Huaping Mo; Andrew A. Bieberich; Alavanja, T.; Colby, a. D. A. Amino-derivatives of the sesquiterpene lactone class of natural products as prodrugs. *MedChemComm.* **2013,** *4*, 27-33.
20. Janganati, V.; Penthala, N. R.; Madadi, N. R.; Chen, Z.; Crooks, P. A. Anti-cancer activity of carbamate derivatives of melampomagnolide B. *Bioorg. Med. Chem. Lett.* **2014,** *24*, 3499-3502.
21. Janganati, V.; Ponder, J.; Jordan, C. T.; Borrelli, M. J.; Penthala, N. R.; Crooks, P. A. Dimers of Melampomagnolide B Exhibit Potent Anticancer Activity against Hematological and Solid Tumor Cells. *J. Med. Chem.* **2015,** *58*, 8896−8906.
22. Penthala, N. R.; Bommagani, S.; Janganati, V.; MacNicol, K. B.; Cragle, C. E.; Madadi, N. R.; Hardy, L. L.; MacNicol, A. M.; Crooks, P. A. Heck products of parthenolide and melampomagnolide-B as anticancer modulators that modify cell cycle progression. *Eur. J. Med. Chem.* **2014,** *85*, 517-525.
23. Baraldi, P. G.; Del Carmen Nunez, M.; Tabrizi, M. A.; De Clercq, E.; Balzarini, J.; Bermejo, J.; Estevez, F.; Romagnoli, R. Design, synthesis, and biological evaluation of hybrid molecules containing alpha-methylene-gamma-butyrolactones and polypyrrole minor groove binders. *J. Med. Chem.* **2004,** *47*, 2877-2886.
24. Ropp, S.; Guy, J.; Berl, V.; Bischoff, P.; Lepoittevin, J. P. Synthesis and photocytotoxic activity of new alpha-methylene-gamma-butyrolactone-psoralen heterodimers. *Bioorg. Med. Chem.* **2004,** *12*, 3619-3625.
25. Ramachandran, P. V.; Pratihar, D.; Nair, H. N.; Walters, M.; Smith, S.; Yip-Schneider, M. T.; Wu, H.; Schmidt, C. M. Tailored alpha-methylene-gamma-butyrolactones and their effects on growth suppression in pancreatic carcinoma cells. *Bioorg. Med. Chem. Lett.* **2010,** *20*, 6620-6623.
26. Jun-Tao, F.; De-Long, W.; Yong-Ling, W.; He, Y.; Xing, Z. New antifungal scaffold derived from a natural pharmacophore: synthesis of alpha-methylene-gamma-butyrolactone derivatives and their antifungal activity against Colletotrichum lagenarium. *Bioorg. Med. Chem. Lett.* **2013,** *23*, 4393-4397.
27. Ramachandran, P. V.; Nicponski, D. R.; Nair, H. N.; Helppi, M. A.; Gagare, P. D.; Schmidt, C. M.; Yip-Schneider, M. T. Synthetic alpha-(aminomethyl)-gamma-butyrolactones and their anti-pancreatic cancer activities. *Bioorg. Med. Chem. Lett.* **2013,** *23*, 6911-6914.
28. Rana, S.; Natarajan, A. Face selective reduction of the exocyclic double bond in isatin derived spirocyclic lactones. *Org. Biomol. Chem.* **2013,** *11*, 244-247.

29. Wen, D.; Nong, Y.; Morgan, J. G.; Gangurde, P.; Bielecki, A.; Dasilva, J.; Keaveney, M.; Cheng, H.; Fraser, C.; Schopf, L.; Hepperle, M.; Harriman, G.; Jaffee, B. D.; Ocain, T. D.; Xu, Y. A selective small molecule IkappaB Kinase beta inhibitor blocks nuclear factor kappaB-mediated inflammatory responses in human fibroblast-like synoviocytes, chondrocytes, and mast cells. *J. Pharmacol. Exp. Ther.* **2006,** *317*, 989-1001.

30. Ploger, M.; Sendker, J.; Langer, K.; Schmidt, T. J. Covalent modification of human serum albumin by the natural sesquiterpene lactone parthenolide. *Molecules* **2015,** *20*, 6211-6223.

31. Bateman, L. A.; Zaro, B. W.; Miller, S. M.; Pratt, M. R. An alkyne-aspirin chemical reporter for the detection of aspirin-dependent protein modification in living cells. *J. Am. Chem. Soc.* **2013,** *135*, 14568-14573.

32. Chen, Q.; Bryant, V. C.; Lopez, H.; Kelly, D. L.; Luo, X.; Natarajan, A. 2,3-Substituted quinoxalin-6-amine analogs as antiproliferatives: a structure-activity relationship study. *Bioorg. Med. Chem. Lett.* **2011,** *21*, 1929-1932.

33. Rajule, R.; Bryant, V. C.; Lopez, H.; Luo, X.; Natarajan, A. Perturbing pro-survival proteins using quinoxaline derivatives: a structure-activity relationship study. *Bioorg. Med. Chem.* **2012,** *20*, 2227-2234.

34. Chaturvedi, N. K.; Rajule, R. N.; Shukla, A.; Radhakrishnan, P.; Todd, G. L.; Natarajan, A.; Vose, J. M.; Joshi, S. S. Novel treatment for mantle cell lymphoma including therapy-resistant tumor by NF-kappaB and mTOR dual-targeting approach. *Mol. Cancer. Ther.* **2013,** *12*, 2006-2017.

35. Gautam, N.; Bathena, S. P.; Chen, Q.; Natarajan, A.; Alnouti, Y. Pharmacokinetics, protein binding and metabolism of a quinoxaline urea analog as an NF-kappaB inhibitor in mice and rats by LC-MS/MS. *Biomed. Chromatogr.* **2013,** *27*, 900-909.

36. Radhakrishnan, P.; Bryant, V. C.; Blowers, E. C.; Rajule, R. N.; Gautam, N.; Anwar, M. M.; Mohr, A. M.; Grandgenett, P. M.; Bunt, S. K.; Arnst, J. L.; Lele, S. M.; Alnouti, Y.; Hollingsworth, M. A.; Natarajan, A. Targeting the NF-kappaB and mTOR pathways with a quinoxaline urea analog that inhibits IKKbeta for pancreas cancer therapy. *Clin. Cancer Res.* **2013,** *19*, 2025-2035.

37. Shao, L.; Wu, L.; Zhou, D. Sensitization of tumor cells to cancer therapy by molecularly targeted inhibition of the inhibitor of nuclear factor kappaB kinase. *Transl. Cancer Res.* **2012,** *1*, 100-108.

38. Mabuchi, S.; Ohmichi, M.; Nishio, Y.; Hayasaka, T.; Kimura, A.; Ohta, T.; Saito, M.; Kawagoe, J.; Takahashi, K.; Yada-Hashimoto, N.; Sakata, M.; Motoyama, T.; Kurachi, H.; Tasaka, K.; Murata, Y. Inhibition of NFkappaB increases the efficacy of cisplatin in in vitro and in vivo ovarian cancer models. *J. Biol. Chem.* **2004,** *279*, 23477-23485.

39. Veiby, O. P.; Read, M. A. Chemoresistance: impact of nuclear factor (NF)-kappaB inhibition by small interfering RNA. Commentary re J. Guo et al., Enhanced chemosensitivity to irinotecan by RNA interference-mediated down-regulation of the NF-kappaB p65 subunit. *Clin. Cancer. Res.* **2004,** *10*, 3262-3264.

40. Chou, T. C. Theoretical basis, experimental design, and computerized simulation of synergism and antagonism in drug combination studies. *Pharmacol. Rev.* **2006,** *58*, 621-681.

41. Rattan, R.; Graham, R. P.; Maguire, J. L.; Giri, S.; Shridhar, V. Metformin suppresses ovarian cancer growth and metastasis with enhancement of cisplatin cytotoxicity in vivo. *Neoplasia* **2011,** *13*, 483-491.

42. Athanassiou, A. E.; Bafaloukos, D.; Pectasides, D.; Dimitriadis, M.; Varthalitis, I.; Barbounis, V. First line combination chemotherapy with cisplatin and etoposide in advanced ovarian cancer. *Br. J. Cancer* **1989,** *60*, 755-758.

43. Meng, F.; Sun, G.; Zhong, M.; Yu, Y.; Brewer, M. A. Anticancer efficacy of cisplatin and trichostatin A or 5-aza-2'-deoxycytidine on ovarian cancer. *Br. J. Cancer* **2013,** *108*, 579-586.

44. Sweeney, C. J.; Mehrotra, S.; Sadaria, M. R.; Kumar, S.; Shortle, N. H.; Roman, Y.; Sheridan, C.; Campbell, R. A.; Murry, D. J.; Badve, S.; Nakshatri, H. The sesquiterpene lactone parthenolide in combination with docetaxel reduces metastasis and improves survival in a xenograft model of breast cancer. *Mol. Cancer Ther.* **2005,** *4*, 1004-1012.

45. Kishida, Y.; Yoshikawa, H.; Myoui, A. Parthenolide, a natural inhibitor of Nuclear Factor-kappaB, inhibits lung colonization of murine osteosarcoma cells. *Clin. Cancer Res.* **2007,** *13*, 59-67.

46. Curry, E. A., 3rd; Murry, D. J.; Yoder, C.; Fife, K.; Armstrong, V.; Nakshatri, H.; O'Connell, M.; Sweeney, C. J. Phase I dose escalation trial of feverfew with standardized doses of parthenolide in patients with cancer. *Invest. New. Drugs* **2004,** *22*, 299-305.

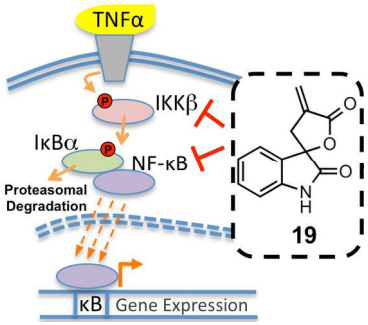
TNFα
IKKβ
IκBα
NF-κB
Proteasomal Degradation
κB
Gene Expression
O
O
O
N
H
19